Catalysis Today 148 (2009) 316–322

Contents lists available at ScienceDirect

Catalysis Today

journal homepage: www.elsevier.com/locate/cattod

ZnO supported on high silica HZSM-5 as new catalysts for dehydrogenation of propane to propene in the presence of CO_2

Yingjie Ren, Fan Zhang, Weiming Hua *, Yinghong Yue *, Zi Gao

Shanghai Key Laboratory of Molecular Catalysis and Innovative Materials, Advanced Materials Laboratory, Department of Chemistry, Fudan University, 220 Handan Road, Shanghai 200433, PR China

ARTICLE INFO

Article history:
Available online 24 June 2009

Keywords:
Propane dehydrogenation
ZnO
High silica HZSM-5
CO_2
Stability

ABSTRACT

Dehydrogenation of propane to propene in the presence of CO_2 was investigated over zinc oxide supported on HZSM-5 with high Si/Al ratios. The stability of supported ZnO catalysts for the reaction improves with increasing the Si/Al ratio of the HZSM-5 support, while the catalytic activity shows a contrary trend. A highly active and stable catalyst, ZnO supported on HZSM-5 with a Si/Al ratio of 160, was obtained, with a propane conversion of 41.5% and a propene yield of 25.8% at steady state. The results of NH_3-TPD and FT-IR spectra of pyridine adsorption reveal that the enhancement of the catalytic stability stems from the decrease in acidity of the catalysts, resulting in the suppression of the side reactions, such as cracking, oligomerization and aromatization. This can be verified by the fact that the amount of coke deposited on the catalyst diminishes with raising the Si/Al ratio of the HZSM-5 support. The promoting effect of CO_2 on the dehydrogenation reaction is observed, which can be attributed to the reverse water-gas shift reaction. The catalytic stability is also enhanced by the introduction of CO_2 to the feed gas.

1. Introduction

Propene is an important raw material for producing polypropene, polyacrylonitrile, acrolein and acrylic acid. The catalytic dehydrogenation of propane to propene has attracted intense attention recently since the propene production from steam cracking and FCC is not sufficient to meet the increasing needs of the market. The present industrial process is not optimal due to the quick deactivation of catalysts during the reaction [1,2]. The oxidative dehydrogenation of propane by oxygen has been proposed as an alternative process. However, the selectivity to propene is relatively low because of the over-oxidation of propane to carbon dioxide in the reaction. Carbon dioxide is a mild oxidant utilized in several partial oxidation reactions, such as reforming and oxidative coupling of methane. The oxidative dehydrogenation of propane by carbon dioxide has also been reported to give rather high propene selectivity. Moreover, carbon dioxide can promote the dehydrogenation reaction by the reversed water-gas shift reaction over supported Cr_2O_3 and Ga_2O_3 catalysts [3–5]. However, the stability of the catalytic reaction is still an unsolved problem, which is fatal for industrial application.

Aromatization of propane over Ga-promoted HZSM-5 catalysts has been studied intensely in the previous decades. The aromatization reaction is thought to proceed via a bifunctional mechanism, in which gallium oxide is responsible for catalyzing the dehydrogenation of propane while Brønsted acid sites account for catalyzing the oligomerization of the olefins thus produced and their subsequent aromatization [6–11]. Our recent work has demonstrated that HZSM-5 supported gallium oxide catalyst was also highly active and stable for the dehydrogenation of propane to propene in the presence of CO_2, when the Si/Al ratio of the HZSM-5 support was increased [12–14]. The high propene yield and superior stability were ascribed to the decrease in the number of acid sites with medium to strong strength on the catalysts, which results in the suppression of the side reactions such as oligomerization, cyclization, cracking and aromatization [13].

Zinc modified HZSM-5 materials with lower Si/Al ratios (generally below 35) are known to be another kind of effective catalysts for the production of aromatics from light alkanes [15,16]. The reaction mechanism is thought to consist of a complex scheme involving dehydrogenation, oligomerization and ring-closure steps. The modifying zinc cations play a key role in the dehydrogenation of light paraffins, which is quite similar to that of gallium species in Ga-promoted HZSM-5 catalysts [17–27]. This suggests that ZnO/HZSM-5 could be also a promising catalyst for the dehydrogenation of propane to propene in the presence of CO_2 if the acidity of the HZSM-5 support is decreased. However, there is little report focused on this so far.

---

* Corresponding authors. Tel.: +86 21 65642409; fax: +86 21 65641740.
E-mail addresses: wmhua@fudan.edu.cn (W. Hua), yhyue@fudan.edu.cn (Y. Yue).

0920-5861/$ – see front matter © 2009 Elsevier B.V. All rights reserved.
doi:10.1016/j.cattod.2009.05.011

In the present work, ZnO catalysts supported on HZSM-5 with high Si/Al ratios were prepared and their catalytic performance for the dehydrogenation of propane to propene in the presence of CO_2 was investigated. The influence of Si/Al ratio of the HZSM-5 support on the catalytic behavior of ZnO/HZSM-5 catalysts as well as the role of CO_2 in the dehydrogenation reaction are also discussed.

2. Experimental

2.1. Catalyst preparation

ZSM-5 zeolites with different Si/Al ratios were prepared following the procedures in the literature [28]. Typically, an aqueous solution of H_2SO_4 was dripped slowly into a solution containing 33.5 g $Na_2SiO_3 \cdot 9H_2O$, calculated amount of $NaAlO_2$, 6.4 g tetrapropylammonium bromide and 56 g H_2O. The pH value is between 8 and 9. After being aged under stirring at room temperature for 4 h, the mixture gel was transferred into a stainless steel autoclave lined with Teflon and crystallized at 180 °C for 2 days. The products were filtered, washed, dried at 100 °C, and finally calcined at 550 °C for 6 h in air. The obtained ZSM-5 zeolites were turned into the H-form by three consecutive ion exchanges with 1 M NH_4NO_3 solution at 80 °C for a total of 9 h and subsequent calcination in air at 550 °C for 6 h.

The supported zinc oxide catalysts were prepared by impregnating an aqueous solution of $Zn(NO_3)_2 \cdot 6H_2O$ on HZSM-5 using an incipient wetness method. The impregnated samples were dried at 100 °C overnight and calcined at 600 °C for 6 h in air. The obtained catalysts are denoted as ZnO/HZSM-5(x), where x represents the molar ratio of Si/Al. The content of ZnO in all the catalysts was 5 wt.%.

2.2. Catalyst characterization

X-ray powder diffraction (XRD) patterns were recorded on a Bruker D8 Advance X-ray diffractometer using nickel-filtered Cu Kα radiation at 40 kV and 40 mA. The bulk Si/Al ratios of the prepared HZSM-5 zeolites were measured by X-ray fluorescence spectrum (XRF) on a Bruker-AXS S4 Explorer. The BET surface areas and micropore volumes of the catalysts were analyzed by N_2 adsorption at −196 °C using a Micromeritics ASAP 2000 instrument. ^{27}Al MAS NMR measurements were performed on a Bruker DSX-300 spectrometer at a resonance frequency of 78.2 MHz. Spectra were recorded at a spinning rate of 12 kHz, a pulse length of 0.31 μs and a delay time of 0.5 s. All the samples were hydrated in a desiccator over a saturated NaCl solution for 3 days prior to the measurements. The surface acidity was measured by temperature-programmed desorption of NH_3 (NH_3-TPD) in a flow-type fixed-bed reactor at ambient pressure. A 100-mg sample was preheated at 550 °C for 2 h, and then cooled to 120 °C in flowing helium. At this temperature, sufficient pulses of ammonia were injected until adsorption saturation occurred, followed by purging with helium for 2 h. The temperature was then raised from 120 to 600 °C at a rate of 10 °C min^{-1}, and the ammonia desorbed was collected in a liquid nitrogen trap and detected by an on-line gas chromatograph (GC) equipped with a TCD. FT-IR spectra of adsorbed pyridine on the catalysts were recorded on a Nicolet Nexus 470 FT-IR spectrometer furnished with an in situ sample cell. A self-supporting disk of the sample (ca. 10 mg) was pretreated at 300 °C for 4 h under a vacuum of 10^{-2} Pa and then cooled to room temperature. FT-IR spectra were recorded after pyridine adsorption at room temperature for 30 min and evacuation at a desired temperature (100–300 °C) for 30 min. Thermal gravimetric analysis (TGA) was conducted in flowing air on a PerkinElmer TGA 7 to determine the amount of coke deposited on the catalyst after reaction.

2.3. Reaction testing

Catalytic tests for propane dehydrogenation were performed at 600 °C in a fixed-bed flow microreactor at atmospheric pressure. The catalyst load was 200 mg, and it was activated at 600 °C for 1 h in nitrogen flow prior to the reaction. The gas reactant contained 2.5 vol% propane, 5 vol% carbon dioxide and balancing nitrogen, unless otherwise stated. The total flow rate of the gas reactant is 20 ml min^{-1}. The hydrocarbon reaction products were analyzed using an on-line GC equipped with a 6-m packed column of Porapak Q and a FID. The gas products, including CO and CO_2, were analyzed on-line by another GC equipped with a 2-m packed column of carbon molecular sieve 601 and a TCD. The reverse water-gas shift reaction on the ZnO/HZSM-5 catalyst was run in the same microreactor at atmospheric pressure. The catalyst load was 200 mg. For the reaction, the total flow rate of the gas reactant is 20 ml min^{-1}, in which $H_2/CO_2/N_2$ molar ratio is 1/1/18. The reaction temperature is in the range of 500–600 °C. The amounts of CO_2 before and after the reaction were analyzed on-line by a GC equipped with a column of carbon molecular sieve 601 and a TCD.

3. Results and discussion

3.1. Catalyst characterization

The HZSM-5 supports with different Si/Al ratios were prepared by a hydrothermal method and their XRD patterns after supporting zinc oxide are shown in Fig. 1. Five diffraction peaks characteristic of MFI structure at $2\theta = 8.0^\circ$, 8.9°, 23.1°, 23.3° and 24.0° are observed on the patterns of all the samples. The peak intensities of the samples are almost the same except for those with Si/Al ratios of 201 and 242, whose crystallinity is slightly lower than that of the others. No characteristic peaks of zinc oxide appeared on the XRD patterns, showing that zinc oxide is well dispersed on the supports.

The composition and textural properties of the supported zinc oxide catalysts are summarized in Table 1. It can be seen that the bulk Si/Al ratio of the HZSM-5 supports measured by XRF is close to that of the initial gel, indicating that the majority of the added Al and Si species is incorporated into the framework of the zeolite during the synthesis. The BET surface areas and micropore volumes of the HZSM-5 supported samples are in the range of 300–344 $m^2\,g^{-1}$ and 0.14–0.16 $cm^3\,g^{-1}$, respectively, showing that the micropore channel of HZSM-5 support was not blocked by the supported ZnO species.

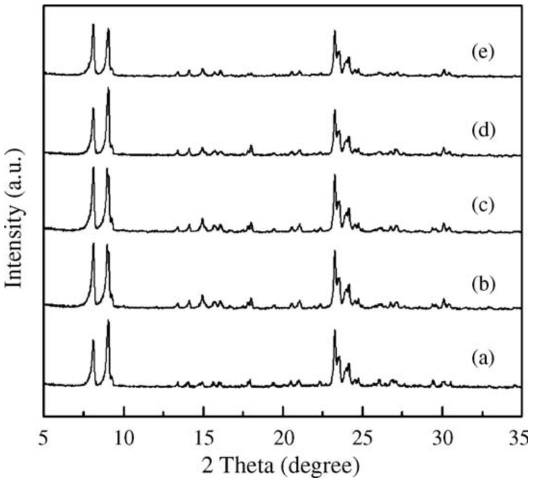

Fig. 1. XRD patterns of the catalysts. (a) ZnO/HZSM-5(60); (b) ZnO/HZSM-5(120); (c) ZnO/HZSM-5(160); (d) ZnO/HZSM-5(201); (e) ZnO/HZSM-5(242).

Table 1
Composition and textural properties of various ZnO/HZSM-5 catalysts.

Catalyst	Si/Al molar ratio		BET area ($m^2\ g^{-1}$)	Micropore volume ($cm^3\ g^{-1}$)
	Reactant gel[a]	Bulk[b]		
ZnO/HZSM-5(60)	60	60	337	0.14
ZnO/HZSM-5(120)	110	120	341	0.15
ZnO/HZSM-5(160)	150	160	312	0.15
ZnO/HZSM-5(201)	200	201	344	0.16
ZnO/HZSM-5(242)	250	242	300	0.15

[a] Calculated from the amounts of $Na_2SiO_3{\cdot}9H_2O$ and $NaAlO_2$ added in the reactant gel.
[b] Determined by XRF.

^{27}Al MAS NMR has been shown to be a powerful technique in the characterization of the local coordination environment of aluminum atoms in zeolites. Fig. 2 depicts the ^{27}Al MAS NMR spectra of the HZSM-5 zeolites with different Si/Al ratios. An intense signal at 54 ppm assigned to 4-coordinate aluminum in the HZSM-5 zeolite framework and a weak one at 0 ppm from extra-framework 6-coordinate aluminum are observed. The intensity of the framework aluminum in all the samples appears much greater than that of extra-framework aluminum, indicating that most of the Al atoms are located in the framework of the zeolite.

3.2. Acidity measurements

The acidity of HZSM-5 supported zinc oxide catalysts was investigated by the NH_3-TPD method, and the results are summarized in Table 2. There is a broad asymmetric NH_3 desorption peak on the TPD profiles of all the supported zinc oxide catalysts (not shown here). NH_3 molecules desorbing between 120 and 350 °C correspond to acidity with weak acid strength, and those desorbing between 350 and 600 °C correspond to acidity with strong acid strength. The number of weak and strong acid sites decreases quickly with increasing the Si/Al ratio of the support from 60 to 201, and diminishes a bit with further increase of the Si/Al ratio from 201 to 242. Similar phenomenon was observed on the Ga_2O_3/HZSM-5 catalysts [14].

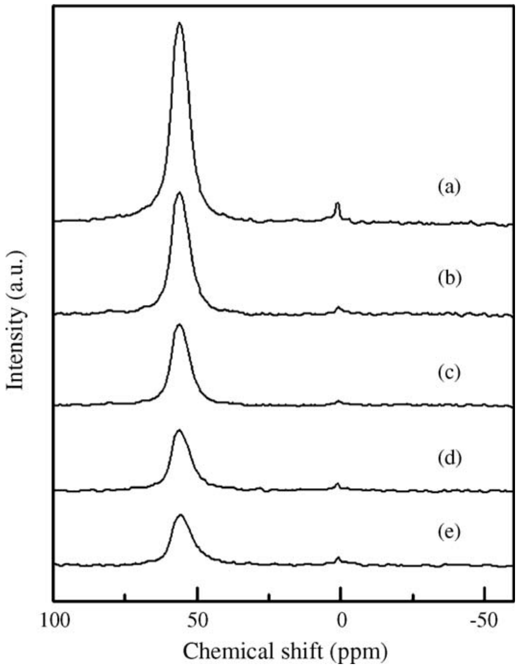

Fig. 2. ^{27}Al MAS NMR spectra of the HZSM-5 supports with different Si/Al ratios. (a) HZSM-5(60); (b) HZSM-5(120); (c) HZSM-5(160); (d) HZSM-5(201); (e) HZSM-5(242).

The nature of the acid sites on HZSM-5 supported ZnO catalysts was measured in situ by FT-IR spectra of adsorbed pyridine on the catalysts. As shown in Fig. 3, the band detected at 1544 cm^{-1} is ascribed to pyridine adsorbed on Brønsted acid sites, whereas the bands assigned to pyridine adsorbed on Lewis acid sites were recorded at 1451 and 1610 cm^{-1}. The band at 1490 cm^{-1} is attributed to pyridine adsorbed on both Brønsted and Lewis acid sites. Brønsted and Lewis acidities are quantified into the integrated areas of the absorbance peaks at 1544 and at 1451 cm^{-1}, respectively, after calibrating the molar extinction coefficients of Brønsted and Lewis acid sites (the ratio of former to latter = 1:1.5 [29]). As presented in Fig. 4, Lewis acidity is much greater than Brønsted acidity for all the catalysts, which results from high Si/Al ratio of the HZSM-5 support and introduction of ZnO to the support. It has been reported that supporting ZnO on HZSM-5 leads to an increased number of Lewis acid sites and a decreased number of Brønsted acid sites [19]. As the Si/Al ratio of the HZSM-5 support increases, the amounts of both Lewis and Brønsted sites decrease, which is consistent with the NH_3-TPD results. When the Si/Al ratio reaches 201 and above, Brønsted acidity is undetectable. This is understandable since the presence of Brønsted sites on HZSM-5 supported zinc oxide catalysts should be directly related to the framework Al species, which is reduced with raising the Si/Al ratio.

3.3. Catalytic performance

Dehydrogenation of propane in the presence of CO_2 was carried out at 600 °C over various HZSM-5 supported zinc oxide catalysts. The results are given in Fig. 5 and Table 3. The initial propane conversion decreases as the Si/Al ratio increases, suggesting that the acidities of the supported zinc oxide catalysts have a great effect on their dehydrogenation activity. ZnO/HZSM-5(60), which is the most acidic one according to the results of NH_3-TPD and FT-IR spectra of adsorbed pyridine, has the highest initial activity. In contrast, the initial propene selectivity increases with raising the Si/Al ratio. As a consequence, the initial propene yield has the sequence of ZnO/HZSM-5(160) > ZnO/HZSM-5(201) > ZnO/HZSM-5(120) > ZnO/HZSM-5(242) > ZnO/HZSM-5(60). For all the catalysts, the propane conversion drops with reaction time and almost reaches

Table 2
NH_3-TPD data of various ZnO/HZSM-5 catalysts.

Catalyst	Amount of desorbed NH_3 (mmol g^{-1})		
	120–350 °C	350–600 °C	Total
ZnO/HZSM-5(60)	0.40	0.41	0.81
ZnO/HZSM-5(120)	0.39	0.27	0.66
ZnO/HZSM-5(160)	0.28	0.21	0.49
ZnO/HZSM-5(201)	0.13	0.11	0.24
ZnO/HZSM-5(242)	0.13	0.10	0.23

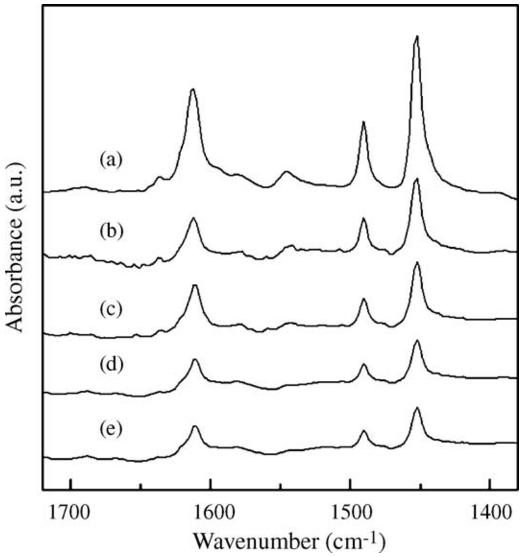

Fig. 3. FT-IR spectra of the catalysts after adsorption of pyridine and desorption at 100 °C. (a) ZnO/HZSM-5(60); (b) ZnO/HZSM-5(120); (c) ZnO/HZSM-5(160); (d) ZnO/HZSM-5(201); (e) ZnO/HZSM-5(242).

steady state in 30 h. The decreasing rate of the catalytic activity becomes lower for those catalysts with Si/Al ratio higher than 160, indicating that the catalyst stability improves as the catalyst acidity decreases. This can also be verified by the coke deposited on the catalysts after reacting for 30 h (Table 3). Noticeably, the ZnO/HZSM-5(160) catalyst gives the best performance, with the highest steady propane conversion (41.5%), the highest steady propene yield (25.8%) and superior stability in the presence of CO_2.

It is widely recognized that the dehydrogenation of light alkanes over zinc-promoted HZSM-5 catalysts proceeds through a bifunctional mechanism. Using DFT calculations, Pidko et al. [27] have proposed more recently that ethane is most likely to be dissociatively adsorbed on zinc oxide sites at the initial step (Eq. (1)), followed by the decomposition of the resulting product via one-step elimination of H_2 and C_2H_4 (Eq. (2)). The activation energy of this elimination reaction is strongly dependent on the relative position of $[Zn–C_2H_5]^+$ and framework attached H^+ ions. Therefore, the presence of acidic protons in the catalyst can promote the regeneration of the active sites, leading to an increase in activity [27].

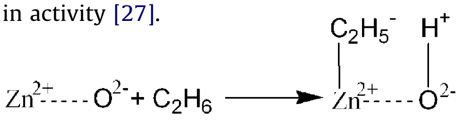

$$Zn^{2+}\text{-----}O^{2-} + C_2H_6 \longrightarrow \overset{C_2H_5^-}{Zn^{2+}}\text{-----}\overset{H^+}{O^{2-}} \qquad (1)$$

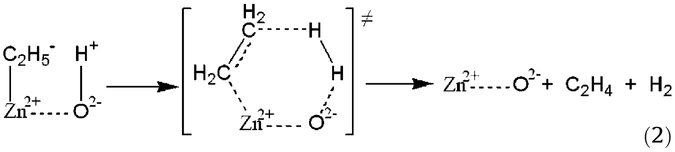

(2)

Similar conclusion could be adopted for the dehydrogenation of propane. As the Si/Al ratio of HZSM-5 support increases, the possibility of occurrence of H^+ ions close to the $[Zn\text{-}C_3H_7]^+$ species in ZnO/HZSM-5 catalyst decreases, resulting in the diminishment of its initial activity. On the other hand, the side reactions, such as cracking, oligomerization and cyclization, also take place on the acid sites. It is well believed that the catalyst deactivation in dehydrogenation reactions is generally attributed to the coke deposition on the catalyst surface. Thus, inhibiting these side reactions through decreasing the number of acid sites present on the catalyst would improve the propene selectivity and the catalyst stability for propane dehydrogenation. This is the reason why the initial selectivity to propene and the catalyst stability are significantly enhanced by reducing the amount of strong acid sites which results from increasing the Si/Al ratio of the HZSM-5 support. Thus, appropriate amount of acid sites is critical for gaining an optimal result, and this goal is achieved in the case of ZnO/HZSM-5(160) in our present study.

3.4. Role of CO_2 in propane dehydrogenation

CO was detected in the reaction products, suggesting that CO_2 was converted into CO during the reaction. It has been reported that CO_2 can react through the reverse water-gas shift reaction and the Boudouard reaction [3–5,30], as shown below:

$$CO_2 + H_2 \rightarrow CO + H_2O \qquad (3)$$

$$CO_2 + C \rightarrow 2CO \qquad (4)$$

In order to understand the role of CO_2 in the reaction, the variation of the amount of CO in the reaction product with reaction time on ZnO/HZSM-5(160) catalyst was tested and given in Fig. 6. The amount of CO formed in the reaction is always higher than that of consumed CO_2, but lower than twice of CO_2 consumed in the reaction, indicating that CO_2 was converted into CO through the above both reactions during the dehydrogenation process.

To gain further information about the role of CO_2 in the dehydrogenation reaction, the effect of CO_2 partial pressure on the dehydrogenation of propane over ZnO/HZSM-5(160) catalyst was investigated, and the results are shown in Fig. 7. The propene yield increases initially with the CO_2/C_3H_8 ratio up to 2, and then decreases with further increasing the CO_2/C_3H_8 ratio. This

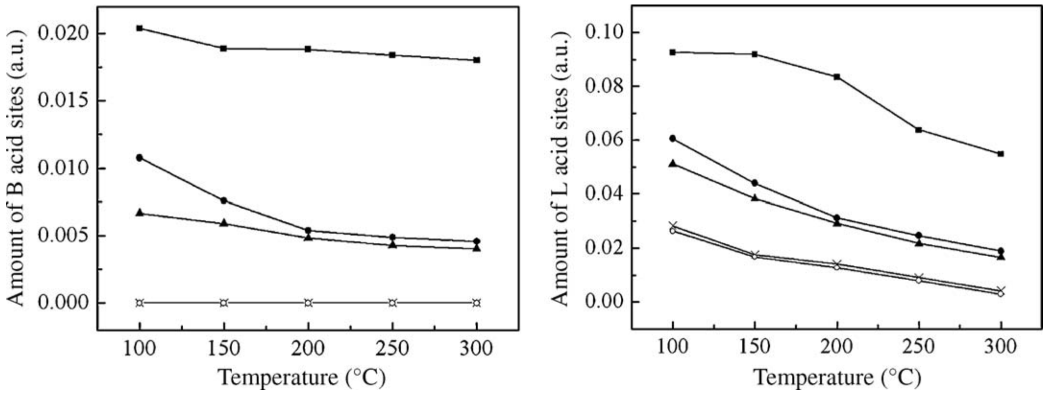

Fig. 4. Amounts of Brønsted (left) and Lewis (right) acid sites of the catalysts at different desorption temperatures. (■) ZnO/HZSM-5(60); (●) ZnO/HZSM-5(120); (▲) ZnO/HZSM-5(160); (×) ZnO/HZSM-5(201); (○) ZnO/HZSM-5(242).

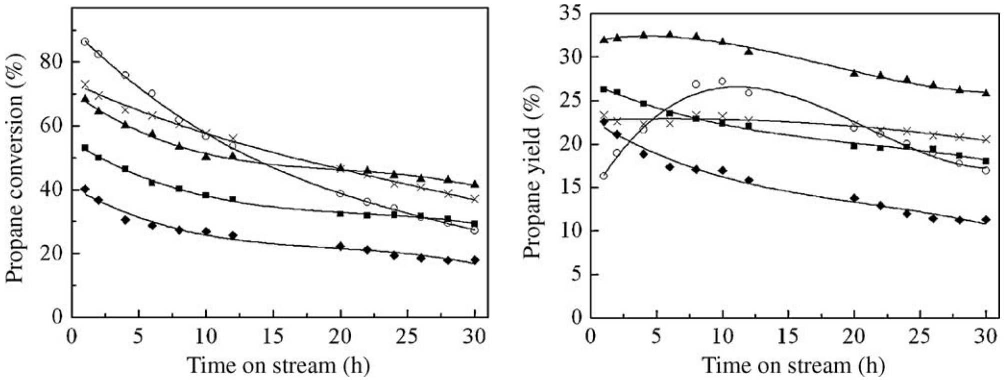

Fig. 5. Propane conversion (left) and propene yield (right) on the catalysts as a function of reaction time. (○) ZnO/HZSM-5(60); (×) ZnO/HZSM-5(120); (▲) ZnO/HZSM-5(160); (■) ZnO/HZSM-5(201); (□) ZnO/HZSM-5(242).

Table 3
Reaction data of the propane dehydrogenation in the presence of CO_2[a].

Catalyst	Conv. (%)[b]	Selectivity (%)					Yield[c]	Coke (wt.%)
		CH_4	C_2H_4	C_2H_6	C_3H_8	Aromatics (%)		
ZnO/HZSM-5(60)	86.2 (27.2)	9.2 (5.7)	8.1 (10.7)	2.7 (0.3)	18.9 (62.3)	61.1 (21.1)	16.3 (16.9)	5.6
ZnO/HZSM-5(120)	73.0 (37.0)	11.4 (6.3)	13.4 (12.0)	3.2 (0.4)	32.0 (55.4)	39.9 (25.8)	23.3 (20.5)	1.3
ZnO/HZSM-5(160)	68.3 (41.5)	6.3 (4.7)	7.0 (7.6)	1.1 (0.3)	46.8 (62.1)	38.8 (25.3)	31.9 (25.8)	1.0
ZnO/HZSM-5(201)	53.1 (29.2)	5.8 (5.0)	10.0 (9.5)	0.8 (0.2)	49.5 (61.8)	33.8 (23.4)	26.3 (18.0)	0.8
ZnO/HZSM-5(242)	40.2 (17.9)	6.3 (6.3)	11.0 (13.0)	0.5 (0.2)	56.1 (63.0)	26.2 (17.6)	22.6 (11.3)	0.7

[a] The values outside and inside the parenthesis are the data obtained at 1 and 30 h, respectively.
[b] Conversion of propane.
[c] Yield of propene.

promoting effect of carbon dioxide on the dehydrogenation reaction can be attributed to the reverse water-gas shift reaction, which accelerates the formation of the dehydrogenation products by transforming H_2 with CO_2 into CO and H_2O [30]. This can be proved by the result of H_2/CO_2 reaction on ZnO/HZSM-5(160), as shown in Fig. 8. Obviously, the ZnO/HZSM-5(150) catalyst is active for the reverse water-gas shift reaction. At 600 °C, the CO_2 conversion reaches 17.4%.

On the other hand, CO_2 has a negative effect on the reaction by displacing the propane adsorbed on the catalyst surface. Propane is thought to be dissociatively adsorbed on zinc oxide [27]. So acidic sites are needed for the adsorption of $C_3H_7^-$, and basic sites are needed for the adsorption of H^+. Since CO_2 is an acidic gas, the competitive adsorption of CO_2 on the basic sites would certainly reduce the possibility of propane adsorption, leading to a reduction in propene yield. The negative effect of CO_2 on the reaction is not so evident at a low concentration of CO_2, and the propene yield increases with increasing the CO_2/C_3H_8 ratio. When the CO_2 concentration further increases, this negative effect becomes dominant and the yield of propene begins to decrease. This accounts for the variation of the propene yield with CO_2/C_3H_8 ratio.

It can also be seen from Fig. 9 that the catalyst stability is greatly improved after the addition of CO_2. The activity of the ZnO/HZSM-5(160) catalyst drops quickly in the absence of CO_2, with an activity loss of 52.7% after 30 h on stream, much greater than 26.8% in the presence of CO_2. This can also be verified by the decrease in amount of coke deposited on the catalyst after reacting in the presence of CO_2 (1.0 wt.%) compared to in the absence of CO_2 (2.4 wt.%). This improvement can be attributed to the suppression of coke formation from two aspects: elimination of coke by the Boudouard reaction and acceleration of desorption of the dehydrogenation product (propene) from the catalyst surface, which was also

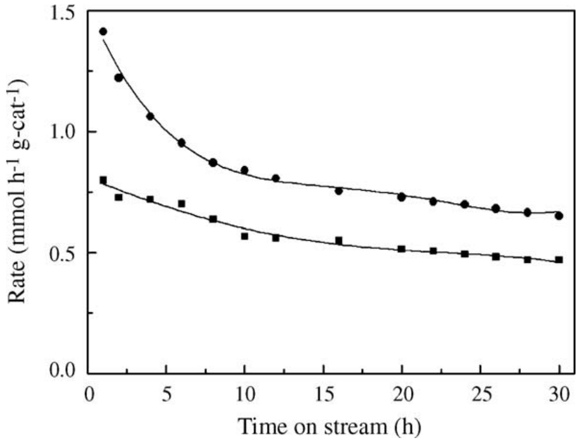

Fig. 6. Rate of CO_2 consumption (■) and CO formation (●) on the ZnO/HZSM-5(160) catalyst at 600 °C.

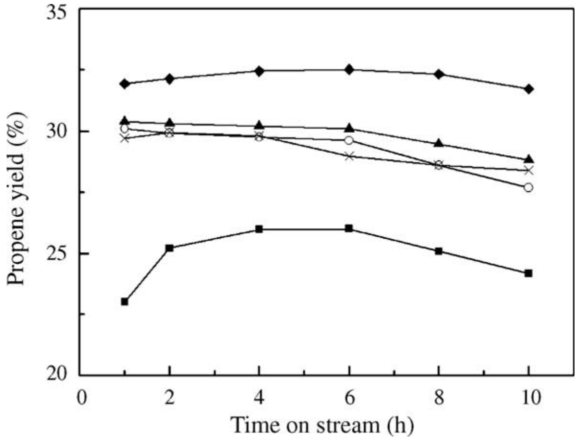

Fig. 7. Effect of CO_2/C_3H_8 ratio on the propene yield over the ZnO/HZSM-5(160) catalyst. CO_2/C_3H_8 ratio equals to: (■) 0; (○) 1; (□) 2; (▲) 4; (×) 6.

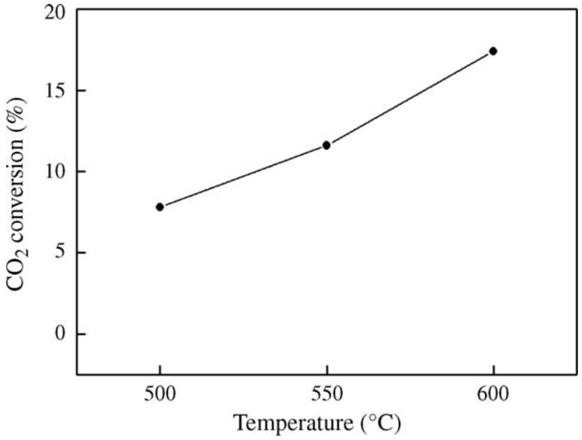

Fig. 8. The result of the reverse water-gas shift reaction on the ZnO/HZSM-5(160) catalyst.

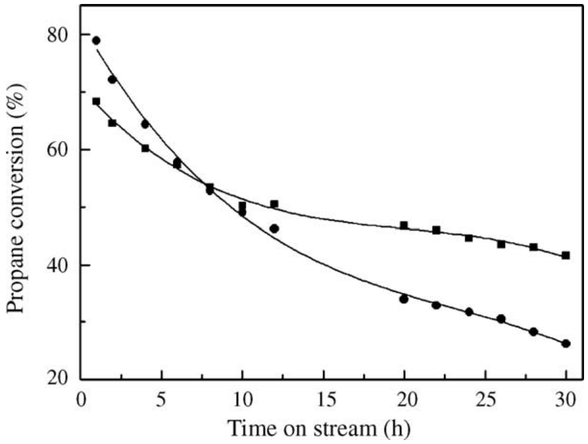

Fig. 9. The stability of the ZnO/HZSM-5(160) catalyst for propane dehydrogenation in the presence (■) and absence (●) of CO_2.

reported for ethane dehydrogenation in the presence of CO_2 over supported Ga_2O_3 catalysts [31].

3.5. Regeneration test

A regeneration treatment of the ZnO/HZSM-5(160) catalyst after 10 h of reaction at 600 °C in the presence of CO_2 was attempted, and the result is shown in Fig. 10. The propane conversion on the catalyst decreases from 68.3% to 50.2% after 10 h on stream. The reaction was interrupted under a N_2 stream, and then O_2 was introduced at 550 °C for 3 h to burn off carbon species deposited on the catalyst. The propane conversion on the regenerated catalyst is 63.3%, which is lower than the initial conversion, showing that the original activity of the catalyst could not be fully restored. Meanwhile, after the second regeneration the activity of the catalyst is almost fully recovered. The increase in the activity after regeneration is owing to the removal of carbonaceous deposit on the catalyst, and the reduction in the activity after the first regeneration could be due to the loss of some temporary active sites on the fresh catalyst.

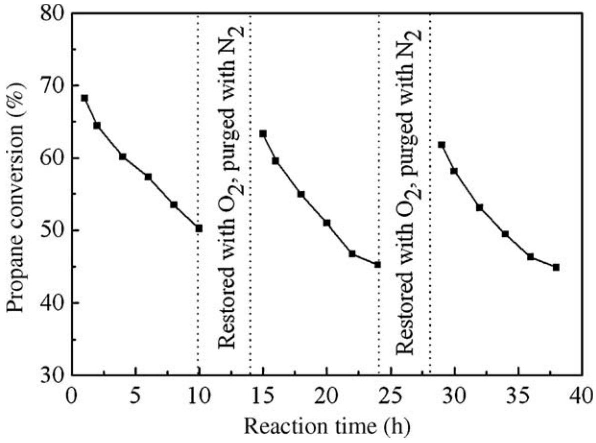

Fig. 10. Regeneration of the ZnO/HZSM-5(160) catalyst at 550 °C.

4. Conclusions

The catalytic dehydrogenation of propane to propene in the presence of CO_2 was carried out over a series of zinc oxide catalysts supported on HZSM-5 with high Si/Al ratios. The initial activity of HZSM-5 supported zinc oxide catalysts decreases with increasing the Si/Al ratio, while the stability and the propene selectivity improve. The ZnO/HZSM-5(160) catalyst exhibits the best performance, with a propane conversion of 41.5% and propene yield of 25.8% at steady state. The enhancement of the catalyst stability with increasing the Si/Al ratio of the HZSM-5 support originates from the decrease in acidity of the catalysts, as revealed by the results of NH_3-TPD and FT-IR spectra of pyridine adsorption, which leads to the suppression of the side reactions, such as cracking, oligomerization and aromatization. The promoting effect of CO_2 on the dehydrogenation reaction is observed over ZnO/HZSM-5 catalyst. Results of the influence of CO_2 partial pressure on the dehydrogenation reaction suggest that there are two roles of CO_2: a positive role by transforming H_2 with CO_2 into CO and H_2O through the reverse water-gas shift reaction, and a negative role by blocking the dissociative adsorption of propane on the catalyst surface. The catalytic stability is also improved by the addition of CO_2 to the feed gas due to the suppression of coke formation.

Acknowledgements

This work was supported by the Chinese Major State Basic Research Development Program (2006CB806103), the National Natural Science Foundation of China (20633030, 20773027 and 20773028) and the Science & Technology Commission of Shanghai Municipality (08DZ2270500).

References

[1] O.A. Barias, A. Holmen, E.A. Blekkan, J. Catal. 158 (1996) 1.
[2] J. Gascón, C. Téllez, J. Herguido, M. Menéndez, Appl. Catal. A 248 (2003) 105.
[3] I. Takahara, M. Saito, Chem. Lett. (1996) 973.
[4] P. Michorczyk, J. Ogonowski, Appl. Catal. A 251 (2003) 425.
[5] B. Zheng, W. Hua, Y. Yue, Z. Gao, J. Catal. 232 (2005) 143.
[6] M. Guisnet, N.S. Gnep, F. Alario, Appl. Catal. A 89 (1992) 1.
[7] H. Himei, M. Yamadaya, M. Kubo, R. Vetrivel, E. Broclawik, A. Miyamoto, J. Phys. Chem. 99 (1995) 12461.
[8] M. Guisnet, N.S. Gnep, Catal. Today 31 (1996) 275.
[9] N.O. Gonzales, A.K. Chakraborty, A.T. Bell, Top. Catal. 9 (1999) 207.
[10] M.V. Frash, R.A. van Santen, J. Phys. Chem. A 104 (2000) 2468.
[11] V.B. Kazansky, I.R. Subbotina, N. Rane, R.A. van Santen, E.J.M. Hensen, Phys. Chem. Chem. Phys. 7 (2005) 3088.
[12] B. Xu, B. Zheng, W. Hua, Y. Yue, Z. Gao, Stud. Surf. Sci. Catal. 170 (2007) 1072.
[13] B. Xu, T. Li, B. Zheng, W. Hua, Y. Yue, Z. Gao, Catal. Lett. 119 (2007) 283.
[14] Y. Ren, W. Hua, Y. Yue, Z. Gao, Chem. J. Chin. Univ. 30 (2009) 1162.
[15] Y. Ono, Catal. Rev.-Sci. Eng. 34 (1992) 179.
[16] A. Hagen, F. Roessner, Catal. Rev.-Sci. Eng. 42 (2000) 403.
[17] M.S. Scurrell, Appl. Catal. 41 (1988) 89.
[18] Y. Ono, K. Kanae, J. Chem. Soc., Faraday Trans. 87 (1991) 669.
[19] H. Berndt, G. Lietz, B. Lücke, J. Völter, Appl. Catal. A 146 (1996) 351.
[20] H. Berndt, G. Lietz, J. Volter, Appl. Catal. A 146 (1996) 365.

[21] N. Viswanadham, A.R. Pradhan, N. Ray, S.C. Vishnoi, U. Shanker, T. Rao, Appl. Catal. A 137 (1996) 225.

[22] J.A. Biscardi, G.D. Meitzner, E. Iglesia, J. Catal. 179 (1998) 192.

[23] J.A. Biscardi, E. Iglesia, J. Catal. 182 (1999) 117.

[24] J. Heemsoth, E. Tegeler, F. Roessner, A. Hagen, Micropor. Mesopor. Mater. 46 (2001) 185.

[25] L.M. Lubango, M.S. Scurrell, Appl. Catal. A 235 (2002) 265.

[26] C.P. Nicolaides, N.P. Sincadu, M.S. Scurrell, Catal. Today 71 (2002) 429.

[27] E.A. Pidko, R.A. van Santen, J. Phys. Chem. C 111 (2007) 2643.

[28] A. Zatta, M.R. Rabaioli, P. Radici, R. Aiello, F. Crea, P. Frontiera, G. Giuffrida, P. Frontera, WO Patent 048188 (2006).

[29] K.H. Rhee, V.U.S. Rao, J.M. Stencel, G.A. Melson, J.E. Crawford, Zeolites 3 (1983) 337.

[30] B. Xu, B. Zheng, W. Hua, Y. Yue, Z. Gao, J. Catal. 239 (2006) 470.

[31] K. Nakagawa, C. Kajita, K. Okumura, N. Ikenaga, M. Nishitani-Gamo, T. Ando, T. Kobayashi, T. Suzuki, J. Catal. 203 (2001) 87.